

Microscopic Dielectric Susceptibility of Germanium

W. COCHRAN

Crystallographic Laboratory, Cambridge, England

AND

J. C. PHILLIPS

Department of Physics, University of Chicago, Chicago, Illinois

(Received 6 January 1964)

The microscopic dielectric susceptibility $\epsilon(q)$ is calculated for germanium using the shell model. It is found that except at $q=0$ the longitudinal and transverse susceptibilities differ and are anisotropic. The results agree qualitatively with Penn's isotropic quantum model based on the random-phase approximation. It is suggested that the quantitative differences may in part represent shortcomings of the RPA in treating the stiffness of covalent bonds.

1. CLASSICAL LATTICE VIBRATION MODELS

MANY classical models have been used to discuss the lattice vibrations of insulators. The interest in such models has been greatly enhanced by the availability of experimentally determined phonon dispersion relations for wavelengths comparable to interatomic separations. Through these models, we may hope to determine certain properties of the valence electron polarizability at short wavelengths.

We may distinguish between two kinds of classical atoms: rigid or polarizable. In each case the valence charge may be regarded as either distributed or localized at a point. For the moment we restrict ourselves to the latter case. The local field corrections in the former case are more involved (Sec. 5).

The rigid point atom yields the simplest models, but is inconsistent with the dielectric properties of ionic crystals. For homopolar Ge, on the other hand, it was natural to suppose that this model would work fairly well. Its failure to fit the dispersion curves determined by inelastic neutron scattering¹ except with forces out to fifth neighbors was shown by Herman.²

Polarizable valence electrons can be treated within the adiabatic approximation as charged massless shells. In a free atom the shell and core are connected by an isotropic force constant; in a crystal each shell is also linked to near neighbor cores and shells. This shell model takes account of the fact that an atom can be polarized either through Coulomb or short-range interactions. In germanium displacement of an atom produces a dipole moment on it, but the lowest moment on the atom and its near neighbors is a quadrupole moment. In Lax's theory³ of the lattice dynamics of germanium, this quadrupole moment is taken to be on the displaced atom; when the shell model is used⁴ the interaction involves the component dipoles. This method finds

some quantum-mechanical justification in the work of Mashkevich and Tolpygo.⁵ It is equivalent to using the atomic displacements and shell displacements (or atomic dipole moments) as generalized coordinates, and writing the energy as a general quadratic form in these coordinates. The shell-shell forces appear formally as the (non-Coulomb) interaction energy of induced dipoles; quantum mechanically they represent the energy required to distort the covalent bonds (Sec. 4).

The microscopic dielectric susceptibility tensor $\epsilon(q)$ is defined by

$$[\epsilon(q) - 1]/4\pi = \mathbf{P}(q)/\mathbf{E}(q). \quad (1.1)$$

Here $\mathbf{E}(q)$ is a macroscopic field of wave number q :

$$\mathbf{E}(q) = \mathbf{E}e^{iq \cdot r} \quad (1.2)$$

and \mathbf{P} is the dipole moment per unit cell volume v

$$v\mathbf{P} = \sum_i \mathbf{p}_i, \quad (1.3)$$

the sum extending over both atoms in the unit cell. For q along $[100]$ or $[111]$ axes in cubic crystals, the tensor $\epsilon(q)$ has only longitudinal and transverse components, $\epsilon_l(q)$ and $\epsilon_t(q)$, respectively.

The shell model gives a good fit⁴ to the experimental lattice vibration spectrum. From this classical model we calculate $\epsilon_t(q)$ in Sec. 2 and $\epsilon_l(q)$ in Sec. 3. Within the Hartree (or random-phase) approximation, one can also calculate $\epsilon(q)$ quantum mechanically (Sec. 4). It follows that $\epsilon(q)$ represents a natural bridge between the experimental dispersion curves and a fundamental quantum-mechanical treatment. The limitations of this approach due to local field and umklapp corrections are discussed in Sec. 5.

2. TRANSVERSE DIELECTRIC SUSCEPTIBILITY

Within the framework of the shell model, this is a purely classical calculation of the microscopic polarization (1.3) produced by the applied field (1.2). We have⁶

$$Y\mathbf{E} = (\mathbf{S}_t + (Y^2/v)\mathbf{C}_t)\mathbf{W}, \quad (2.1)$$

⁵ V. S. Mashkevich and K. B. Tolpygo, *Zh. Eksperim. i Teor. Fiz.* **32**, 520 (1957) [English transl.: *Soviet Phys.—JETP* **5**, 435 (1957)].

⁶ W. Cochran, *Advan. Phys.* **10**, 401 (1961).

¹ B. N. Brockhouse and P. K. Iyengar, *Phys. Rev.* **111**, 747 (1958); A. Ghose, H. Palevsky, D. J. Hughes, I. Pelah, and C. M. Eisenhauer, *ibid.* **113**, 49 (1959).

² F. Herman, *Phys. Chem. Solids* **8**, 405 (1959).

³ M. Lax, *Phys. Rev. Letters* **1**, 133 (1958); *Phys. Chem. Solids* **8**, 422 (1959).

⁴ W. Cochran, *Proc. Roy. Soc. (London)* **A253**, 260 (1959).

where Y is a constant equal to the charge on a shell. The applied electric field and dipole moments at the two atoms in the unit cell are vector elements of the column matrices \mathbf{E} and $Y\mathbf{W}$. (The elements of \mathbf{E} are therefore equal.) The short-range and Coulomb forces are represented by the 2×2 matrices \mathbf{S}_t and \mathbf{C}_t , respectively. Because we are taking \mathbf{q} along a $[111]$ or $[100]$ symmetry direction, and $\mathbf{E} \perp \mathbf{q}$, the matrix elements of \mathbf{S}_t and \mathbf{C}_t are scalar functions of q . For example, for $q \rightarrow 0$ all four elements of \mathbf{C} have the value $-\frac{4}{3}\pi$. Different scalar functions enter for $\mathbf{E} \parallel \mathbf{q}$, so that $\epsilon_t(\mathbf{q})$ calculated here differs from $\epsilon_l(\mathbf{q})$ calculated in the next section.

According to these definitions we can write the polarization (1.3) as

$$v\mathbf{P} = Y\mathbf{W} \quad (2.2)$$

and from (2.1) and (2.2) it follows that

$$\mathbf{P} = ((v\mathbf{S}_t/Y^2) + \mathbf{C}_t)^{-1}\mathbf{E}. \quad (2.3)$$

Since for the Ge lattice the off-diagonal matrix elements of $(v\mathbf{S}_t/Y^2 + \mathbf{C}_t)$ are complex conjugates, the polarization waves through the two types of atom are not in phase with the applied field \mathbf{E} . Because the matrix is Hermitian, one lags as much as the other leads. We may take the sum of the two to define a real microscopic dielectric susceptibility given by

$$\epsilon_{st}(\mathbf{q}) = 1 + 4\pi \sum ((v\mathbf{S}_t/Y^2) + \mathbf{C}_t)^{-1}, \quad (2.4)$$

where the sum is over all four elements of the matrix.

We can check the correctness of this procedure by evaluating (2.4) at $q=0$. In this limit the shell-shell forces do not affect the polarizability, which depends only on core-shell forces. We find that in terms of the free atom polarizability per unit cell volume β (2.4) reduces to

$$[\epsilon_{st}(0) - 1]/[\epsilon_{st}(0) + 2] = \frac{4}{3}\pi\beta, \quad (2.5)$$

which is the Clausius-Mossotti formula.^{4,7} Thus (2.4) includes local field corrections properly when the valence electrons are idealized as nonoverlapping spherical shells.

Using the values of \mathbf{C}_t and \mathbf{S}_t given previously in Table III and Appendix 4, respectively,⁴ one can now evaluate (2.4) along the $[100]$ and $[111]$ axes. The results are shown in Figs. 1 and 2.

A notable feature of these curves is their periodicity, which is not that of the reduced Brillouin zone. The periodicity is a result of the localization of the two valence shells on the atoms rather than merely in the unit cell. We also note that $\epsilon_{st}(q)$ along the $[111]$ direction has a maximum near $\mathbf{q} = \bar{K} = 2\pi a^{-1}(111)$. This may be an umklapp effect (Sec. 5).

⁷ The value of β used here is 0.099, which gives $\epsilon(0) = 16.0$. It differs slightly from the value of 0.105 used in Ref. 4.

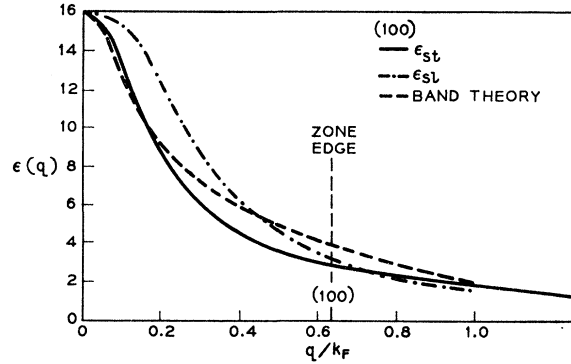


FIG. 1. The longitudinal and transverse shell-model susceptibilities ϵ_{sl} and ϵ_{st} , respectively, as a function of q/k_F along $[100]$ axes, where k_F is the Fermi wave number of a free-electron gas of density equal to the valence electron density in Ge. The curve marked band theory is based on Penn's isotropic band model.

3. LONGITUDINAL SUSCEPTIBILITY

In this case we have

$$Y\mathbf{E} = (\mathbf{S}_l + (Y^2/v)\mathbf{C}_l)\mathbf{W}, \quad (3.1)$$

where as before the elements of the matrix \mathbf{E} are the amplitude of the applied field. The effective field is the sum of the applied, local and macroscopic fields, the two latter being given by $-(Y/v)\mathbf{C}_l\mathbf{W}$. That is, the local and macroscopic fields are not calculated separately by Kellermann's method.⁸ At $q \rightarrow 0$, for example, the elements of \mathbf{C}_l are all $8\pi/3$. The amplitude of the macroscopic field is -4π times the amplitude of the polarization wave, and this is true for general values of q .⁹

Let P be the amplitude of the polarization wave, E that of the applied field and $E_M = -4\pi P$ that of the macroscopic field. We define $\epsilon_l(q)$ by

$$[\epsilon_l(q) - 1]/4\pi = P/(E + E_M),$$

so that

$$[\epsilon_l(q) - 1]/4\pi\epsilon_l(q) = P/E. \quad (3.2)$$

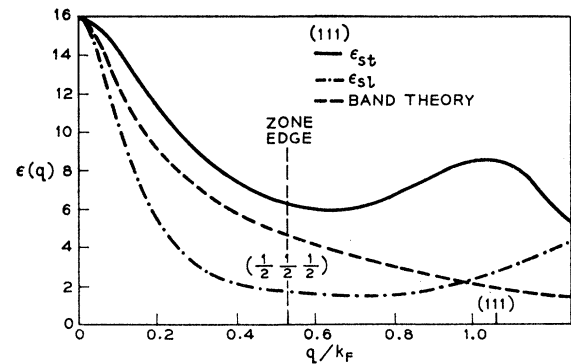


FIG. 2. The same as Fig. 1, but with \mathbf{q} parallel to $[111]$.

⁸ E. W. Kellerman, Phil. Trans. Roy. Soc. (London) **A238**, 513 (1940).

⁹ M. Born and K. Huang, *Dynamical Theory of Crystal Lattices* (Oxford University Press, New York, 1954).

By the same argument as was given in the previous section, we then have

$$\frac{\epsilon_l(q)-1}{4\pi\epsilon_l(q)} = \sum \left(\mathbf{S}_l \frac{v}{Y^2} + \mathbf{C}_l \right)^{-1}. \quad (3.3)$$

Making use of the fact that if

$$(\epsilon-1)/4\pi = \sum \mathbf{X}^{-1},$$

then

$$(\epsilon-1)/4\pi\epsilon = \sum (\mathbf{X} - 4\pi\mathbf{I})^{-1},$$

where

$$\mathbf{I} = \begin{pmatrix} 1 & \\ & 1 \end{pmatrix}.$$

We finally have

$$\epsilon_l(q) = 1 + 4\pi \sum (\mathbf{S}_l(v/Y^2) + \mathbf{C}_l - 4\pi\mathbf{I})^{-1}. \quad (3.4)$$

The elements of \mathbf{C}_l and of \mathbf{C}_t are related by⁸

$$\mathbf{C}_l + 2\mathbf{C}_t = 0. \quad (3.5)$$

It is readily verified from (2.4), (3.4), and (3.5), together with the fact that $s_t(0) = s_l(0)$, that $\epsilon_l(0) = \epsilon_t(0)$ (as required by cubic symmetry).

Using the expressions for \mathbf{S} appropriate to longitudinal modes,⁴ we have evaluated (3.5) along the [100] and [111] symmetry directions. The results are shown in Figs. 1 and 2, where they are compared with $\epsilon_{st}(q)$. Except at $q=0$ (where shell-shell forces play no role), $\epsilon_{st}(\mathbf{q})$ is not equal to $\epsilon_{st}(\mathbf{q})$; the difference is small along the [100] direction where \mathbf{q} makes equal angles with all shell-shell force constants, and large along [111] directions where \mathbf{q} is parallel to one of the shell-shell force constants.

The idea that shell-shell forces are chiefly responsible for the difference between $\epsilon_{st}(\mathbf{q})$ and $\epsilon_{st}(\mathbf{q})$ is borne out by the explicit expressions⁴ for $-S/S_0$. These are

$$[100] \text{ trans. } \cos qa/4 - i\gamma_s \sin qa/4, \quad (3.6)$$

$$[100] \text{ long. } \cos qa/4, \quad (3.7)$$

$$[111] \text{ trans. } \cos^3\theta + \gamma_s \sin^2\theta \cos\theta + i(\sin^3\theta + \gamma_s \cos^2\theta \sin\theta), \quad (3.8)$$

$$[111] \text{ long. } \cos^3\theta - 2\gamma_s \sin^2\theta \cos\theta + i(\sin^3\theta - 2\gamma_s \cos^2\theta \sin\theta), \quad (3.9)$$

where $\theta = qa/4\sqrt{3}$. With $\gamma_s = 0$ the longitudinal and transverse short-range forces become equal. The parameter γ_s measures⁴ the ratio of transverse to longitudinal shell-shell forces along cube axes:

$$\gamma_s = [\phi_{xy}(s-s)]/[\phi_{xx}(s-s)], \quad (3.10)$$

where ϕ_{xy} is proportional to the force in the x direction on shell 1 when shell 2 is displaced in the y direction. The value of γ_s used previously⁴ was 0.7.

One can express γ_s in terms of the ratio of bond bending to bond stretching forces. One obtains

$$\gamma_s = (k_s - k_B)/(k_s + 2k_B). \quad (3.11)$$

Thus, $\gamma_s = 0.7$ corresponds to $k_B/k_s = 0.13$. This is in quantitative agreement with the ratio of core-core and core-shell bond bending and bond stretching forces required to fit the elastic constants⁴ and other theoretical¹¹ and experimental data¹² in the $q=0$ limit.

4. QUANTUM-MECHANICAL SUSCEPTIBILITY

In treating the real crystal quantum mechanically, we are concerned with fields throughout the unit cell and not merely at the atomic sites. If the external potential is $v(x)$ and the self-consistent total potential is $V(x')$, we have the general relation

$$v(x) = - \int_{\Omega} \mathfrak{D}(x, x') V(x') dx'. \quad (4.1)$$

Here the integral extends over the volume of the crystal.

The microscopic dielectric susceptibility is $\mathfrak{D}(x, x')$. When (4.1) is Fourier analyzed, taking advantage of periodicity, one obtains¹³⁻¹⁵

$$v(\mathbf{q}, \mathbf{K}_p) = \sum_{p'} \mathfrak{D}(\mathbf{q}, \mathbf{K}_p, \mathbf{K}_{p'}) V(\mathbf{q}, \mathbf{K}_{p'}). \quad (4.2)$$

We are interested in the case $\mathbf{K}_p = 0$. Then (4.2) may be rewritten

$$v(q, 0) = \epsilon(q) V(q) + \sum_{p'} \mathfrak{D}(\mathbf{q}, 0, \mathbf{K}_{p'}) V(\mathbf{q}, \mathbf{K}_{p'}), \quad (4.3)$$

where the prime on the summation excludes $\mathbf{K}_{p'} = 0$.

We have chosen to regard $\epsilon(q)$, the $\mathbf{K}_p = \mathbf{K}_{p'} = 0$ component of the operator \mathfrak{D} , as the quantum-mechanical analog of $\epsilon_s(q)$. Because of the point nature of the shell model, this choice is not unique. We shall see in Sec. 5 that with this choice the local field corrections to $\epsilon(q)$ associated with a distributed shell charge are small, at least within the first Brillouin zone. We also postpone to Sec. 5 the discussion of the second set of terms on the right of (4.3), which may be called umklapp corrections.

If one knows one-electron wave functions and energies throughout the Brillouin zone, $\epsilon(q)$ may be calculated using the random-phase approximation¹⁶ (RPA). For the static dielectric function we are considering,

$$\epsilon(\mathbf{q}) = 1 + \frac{1}{N} \sum_n \frac{f_{0n}(\mathbf{q}) \omega_p^2}{\omega_n^2}. \quad (4.4)$$

The oscillator strengths $f_{0n}(\mathbf{q})$ are, in general, different for longitudinal and transverse polarizations; they are

¹⁰ A. D. B. Woods, W. Cochran, and B. N. Brockhouse, Phys. Rev. **119**, 980 (1960).

¹¹ L. Kleinman, Phys. Rev. **128**, 2614 (1962).

¹² A. Segmuller, Phys. Letters **4**, 277 (1963).

¹³ S. L. Adler, Phys. Rev. **126**, 413 (1962).

¹⁴ N. Wiser, Phys. Rev. **129**, 62 (1963).

¹⁵ M. Azuma, J. Phys. Soc. Japan **18**, 194 (1963).

¹⁶ P. Nozieres and D. Pines, Phys. Rev. **109**, 762 (1958).

the same only in the case of an isotropic solid such as a free-electron gas.

An isotropic model of a semiconductor has been studied by Penn.¹⁷ The model contains an energy gap between the valence and conduction bands. Near this gap the Bloch functions are made out of two plane waves, \mathbf{k} and $\mathbf{k}-\mathbf{K}$. The "reciprocal lattice vectors" \mathbf{K} involved are always parallel to \mathbf{k} . The umklapp terms are negligible, being of order N^{-1} , where N is the number of atoms in the crystal. The model also makes the longitudinal and transverse dielectric susceptibilities equal. This result may apply more generally than merely to Penn's model. That is, the anisotropy of $\epsilon(\mathbf{q})$ may be a measure of the magnitude of umklapp corrections.

Penn shows that a dielectric susceptibility consistent with his band model is given by the formula

$$\epsilon(q) = 1 + \left(\frac{\hbar\omega_p}{E_g} \right)^2 \frac{1}{[1 + (E_F/E_g)(q/k_F)^2]}. \quad (4.5)$$

Here E_F and k_F are the Fermi energy and wave number of the valence electrons regarded as a free-electron gas. With $E_F = 12$ eV, $E_g = 4$ eV, (4.5) reduces to

$$\epsilon(q) = 1 + \frac{15}{[1 + 3.0(q/k_F)^2]}. \quad (4.6)$$

We have called (4.6) the dielectric function obtained from band theory. It is also plotted in Figs. 1 and 2.

We see that along the [100] axis, where the difference between ϵ_{st} and ϵ_{sl} is small, $\epsilon(q)$ from (4.6) agrees well with ϵ_s . This confirms our identification of $\epsilon(\mathbf{q})$ with the $\mathbf{K}_p=0$ component of $\mathfrak{D}(\mathbf{q}, \mathbf{K}_p)$. That the agreement of a classical model with point charges with a quantum-mechanical band model should be so good is at first unexpected. We are less surprised, however, when we remember that the shell model gives a good fit to the neutron data in a rather simple way.

Along the [111] axis, ϵ_{st} differs substantially from ϵ_{sl} , even within the zone. (At the zone edge, $\epsilon_{st} \approx 3\epsilon_{sl}$). Within the zone, ϵ falls between ϵ_{sl} and ϵ_{st} . We now wish to consider whether the large difference between ϵ_{st} and ϵ_{sl} is real, and if so, what shortcoming of the band model makes the difference zero there.

To answer this question we must discuss the quantum-mechanical equivalent of the parameter γ_s . According to (3.11), $S_0\gamma_s$ increases with k_{ss} , the force constant involved in stretching the covalent bond. The tendency of shell-core forces is to pull the valence charge distributions apart; it is necessary to balance this with a bond stretching force. Quantum mechanically, bond stretching causes a substantial lowering of valence charge density near the covalent plane, defined as the plane midway between the two atoms in the unit cell. This requires an increase in kinetic energy, which

is represented by the shell-shell force constant. The charge density at the covalent plane is little altered by bond bending so that $k_s \ll k_s$.

We can now see that the quantum-mechanical generalization of the bond stretching force constant k_s is a force distributed over the covalent face of the atomic cell and acting on a distributed and deformable valence shell. The effect of these refinements should be to reduce the differences between ϵ_{st} and ϵ_{sl} along the [111] axes, perhaps by 50%, but not eliminate them altogether.

It would be interesting to know whether a realistic band model would produce a substantial difference between ϵ_{st} and ϵ_{sl} . From previous experience¹⁸ with $\epsilon(q)$ at $q=0$, it appears that much ingenuity would be required to carry out calculations for $q \neq 0$. It also appears that with many bands, the tendency towards isotropy within the random-phase approximation (4.3) is strong. We suspect that the anisotropy manifested in Fig. 2 indicates that covalent bonding involves short-range correlations which are not treated accurately by the RPA.

5. LOCAL FIELD AND UMKLAPP CORRECTIONS

It was remarked in Sec. 2 that $\epsilon_s(q)$ is periodic along [100] and [111] axes. If we replace a point shell at \mathbf{R} by a specified charge distribution $\sigma(\mathbf{r}-\mathbf{R})$, we find that the force on a shell is

$$\mathbf{E} \int e^{i[\mathbf{q} \cdot (\mathbf{R} + \mathbf{r})]} \sigma(\mathbf{r}) d^3\mathbf{r}. \quad (5.1)$$

This is just the previous value, multiplied by the form factor of $\sigma(\mathbf{r})$, which we write as

$$Y(\mathbf{q}) = \int \sigma(\mathbf{r}) e^{i\mathbf{q} \cdot \mathbf{r}} d^3\mathbf{r}. \quad (5.2)$$

On Fourier analyzing the polarization one finds, e.g., for ϵ_{st} ,

$$\frac{\epsilon_{st}(q) - 1}{4\pi} = \frac{Y^2(q)}{Y^2(0)} \sum \left(\frac{v\mathbf{S}_t}{Y^2} + \mathbf{C}_t \right)^{-1}. \quad (5.3)$$

When an extended charge distribution is used the elements of \mathbf{C}_t will not be the same as those we have met previously, which apply to charges localized at a point (or to nonoverlapping spherical distributions). For example, as the charge is spread out, $C_t(0)$ changes from $-4\pi/3$ to zero, and $C_t(0)$ from $+8\pi/3$ to $+4\pi$. However these changes can be taken up in \mathbf{S} , in other words it will always be possible to keep $(v\mathbf{S}/Y^2) + \mathbf{C}$ unchanged. Thus with this quantity unchanged, so that the phonon dispersion curves are unchanged, the right-hand side of (5.3) is multiplied by the damping factor $Y^2(q)/Y^2(0)$ compared to (2.4).

¹⁷ D. Penn, Phys. Rev. **128**, 2093 (1962).

¹⁸ D. Brust, J. C. Phillips, and F. Bassani, Phys. Rev. Letters **9**, 89 (1962).

By comparing $\epsilon_s(q)$ with $\epsilon(q)$, we can see that the damping factor must be nearly 1 within the Brillouin zone and start to decrease rapidly for $q \gtrsim k_p$. Outside the zone $\epsilon_s(q)$ represents an analytic continuation of the susceptibility which gives a good fit to that deduced from the phonon dispersion curves inside the zone. The continuation is not unique, as we see from the presence of the damping factor in (5.3). Nevertheless, the damping is probably not so rapid as to destroy the maxima in ϵ_{st} and ϵ_{st} for \mathbf{q} near $\mathbf{L}=[111]$ reciprocal lattice vector.

Such maxima can be called umklapp effects. Azuma¹⁵ has shown that the umklapp terms in (4.2) lead to an effect of this sort. He finds

$$\epsilon(\mathbf{K}_p) = \mathfrak{D}(\mathbf{K}_p, 0) / [1 - C_p / \epsilon(0)], \quad (5.4)$$

where C_p is a number of order unity. The enhancement predicted by (5.4) may be related to the subsidiary maxima found in ϵ_s for \mathbf{q} near \mathbf{L} .

6. CONCLUSIONS

In spite of the differences between a classical model of point valence shells and a quantum-mechanical model with valence charge spread over the atomic cell, the microscopic dielectric susceptibility obtained from the shell model is in qualitative agreement with the RPA result, especially within the zone. This provides some microscopic justification of the shell model.

Lax¹⁹ has criticized the shell model on the grounds that its point nature grossly overemphasizes the local field corrections. He cites Stark shifts of nuclear resonances,²⁰ which place an upper limit on the corrections

¹⁹ M. Lax, 1963 Copenhagen Conference on Lattice Dynamics (to be published).

²⁰ N. Bloembergen, *Proceedings of the Eindhoven Conference on Magnetic and Electric Resonance and Relaxation* (North-Holland Publishing Company, Amsterdam, 1963), p. 39.

of order 50%, whereas the point charge model implies corrections by a factor $(\epsilon+2)/3 \sim 5$, i.e., ten times larger than the experimental shifts.

Our calculations here demonstrate how the shell model overcomes these difficulties. The microscopic susceptibility calculated from band theory, $\epsilon(q)$, implies small (or, in the case of the isotropic model, no) local field corrections. Nevertheless $\epsilon_s(q)$ agrees well with $\epsilon(q)$ near the zone edge. This is because the short-range forces dominate both the lattice vibration frequencies and $\epsilon_s(q)$ in this region. As $q \rightarrow 0$ phase differences between nearest neighbors are reduced, the short-range forces are reduced, and the long-range Coulomb forces become important. In this limit the nature of the charge distribution in the unit cell is irrelevant, so long as it is treated *consistently* to give the right limit,

$$\lim_{q \rightarrow 0} \epsilon_{st}(q) = \lim_{q \rightarrow 0} \epsilon_s(q) = \epsilon_0 = 16, \quad (6.1)$$

for the dielectric properties. This the shell model does; adjustment of β to give $\epsilon_0=16$ automatically renormalizes the theory.

We can now reverse this argument and use the fact that short-range forces dominate near the zone edge to argue that the differences between $\epsilon_{st}(q)$ and $\epsilon_s(q)$ along $[111]$ axes are real. These differences may represent the first observable evidence for departures from the RPA in metals or semiconductors.

ACKNOWLEDGMENTS

One of us (J. C. P.) has benefited from conversations with M. Lax. Part of this work was carried out by J. C. P. as a Guggenheim fellow with a Sloan grant in aid at Cambridge, and part at Bell Laboratories.